

AD-A242 570



REPORT DOCUMENTATION PAGE

1991  
E  
D

2b. DECLASSIFICATION / DOWNGRADING SCHEDULE		1b. RESTRICTIVE MARKINGS	
4. PERFORMING ORGANIZATION REPORT NUMBER(S) Report #2		3. DISTRIBUTION / AVAILABILITY OF REPORT Approved for public release; distribution unlimited	
6a. NAME OF PERFORMING ORGANIZATION Washington University	6b. OFFICE SYMBOL (if applicable)	7a. NAME OF MONITORING ORGANIZATION Office of Naval Research	
6c. ADDRESS (City, State, and ZIP Code) One Brookings Drive St. Louis, MO 63130-4899		7b. ADDRESS (City, State, and ZIP Code) 800 N. Quincy Street Arlington, VA 22217-5000	
8a. NAME OF FUNDING / SPONSORING ORGANIZATION ONR	8b. OFFICE SYMBOL (if applicable)	9. PROCUREMENT INSTRUMENT IDENTIFICATION NUMBER N00014-90-J-4118; R&T Code (413M001)	
8c. ADDRESS (City, State, and ZIP Code) 800 N. Quincy Street Arlington, VA 22217-5000		10. SOURCE OF FUNDING NUMBERS	
		PROGRAM ELEMENT NO.	PROJECT NO.
		TASK NO.	WORK UNIT ACCESSION NO.
11. TITLE (Include Security Classification) Mechanism of DNP-Enhanced Polarization Transfer Across the Interface of Polycarbonate/Poly-styrene Heterogeneous Blends			
12. PERSONAL AUTHOR(S) Mobaef Afeworki and Jacob Schaefer			
13a. TYPE OF REPORT Technical	13b. TIME COVERED FROM _____ TO _____	14. DATE OF REPORT (Year, Month, Day) 11/14/91	15. PAGE COUNT 29
16. SUPPLEMENTARY NOTATION			
17. COSATI CODES		18. SUBJECT TERMS (Continue on reverse if necessary and identify by block number)	
FIELD	GROUP	SUB-GROUP	
		Interface-PC; thin-film blends; DNP-difference; PC/PS interface.	
19. ABSTRACT (Continue on reverse if necessary and identify by block number)			
<p>The same integrated intensity is observed for the interface-PC signal in PC(<sup>13</sup>C)/PS(<sup>12</sup>C/*) and PC(<sup>13</sup>C)/PS(<sup>2</sup>D/*) thin-film blends in a DNP-difference experiment. This result proves that the dominant mechanism of polarization transfer from the electrons in the PS phase to the protons in the PC phase is by direct polarization transfer. The interface-PC signal intensity arises from a 60-Å region which is 2* of the PC film thickness. Minor polarization transfer from the DNP-enhanced protons of PS to the PC protons across the PC/PS interface via H-H spin-diffusion in PC(<sup>13</sup>C)/PS(<sup>12</sup>C/*) may also occur. Even in BDPA-doped homopolymers, the enhancement mechanism is mainly via direct solid-effect polarization transfer, a conclusion based on the similarity of the time dependence of the electron-proton polarization transfers for PS(*) and PS(<sup>2</sup>D/*).</p>			
20. DISTRIBUTION / AVAILABILITY OF ABSTRACT <input checked="" type="checkbox"/> UNCLASSIFIED/UNLIMITED <input type="checkbox"/> SAME AS RPT <input type="checkbox"/> DTIC USERS		21. ABSTRACT SECURITY CLASSIFICATION	
22a. NAME OF RESPONSIBLE INDIVIDUAL Dr. Jacob Schaefer	22b. TELEPHONE (Include Area Code) 314-935-6844	22c. OFFICE SYMBOL	

## II. Mechanism of DNP-Enhanced Polarization Transfer Across the Interface of Polycarbonate/Polystyrene Heterogeneous Blends

Mobae Afeworki† and Jacob Schaefer

Department of Chemistry  
Washington University  
St Louis, MO 63130

Accession For	
NTIS GRA&I	<input checked="" type="checkbox"/>
DTIC TAB	<input type="checkbox"/>
Unannounced	<input type="checkbox"/>
Justification	
By _____	
Distribution/	
Availability Codes	
Dist	Avail and/or Special
A-1	

†Present Address: Exxon Research and Engineering Company, Annandale, NJ  
08801

91-15772



## ABSTRACT

The same integrated intensity is observed for the interface-PC signal in PC( $^{13}\text{C}$ )/PS( $^{12}\text{C}/*$ ) and PC( $^{13}\text{C}$ )/PS( $^{2}\text{D}/*$ ) thin-film blends (see previous paper for sample notation) in a DNP-difference experiment. This result proves that the dominant mechanism of polarization transfer from the electrons in the PS phase to the protons in the PC phase is by direct polarization transfer. The interface-PC signal intensity arises from a 60-Å region which is 2% of the PC film thickness. Minor polarization transfer from the DNP-enhanced protons of PS to the PC protons across the PC/PS interface via H-H spin-diffusion in PC( $^{13}\text{C}$ )/PS( $^{12}\text{C}/*$ ) may also occur. Even in BDPA-doped homopolymers, the enhancement mechanism is mainly via direct solid-effect polarization transfer, a conclusion based on the similarity of the time dependence of the electron-proton polarization transfers for PS( $*$ ) and PS( $^{2}\text{D}/*$ ).

## INTRODUCTION

The DNP-enhanced PC-interface signal of Figure 12 (top,  $\delta_C$  120) of the previous paper (I) was obtained by a double-polarization transfer: electrons to protons to carbons. In this paper, we report the time dependence of the first transfer, electrons to protons, and discuss whether this solid-effect transfer is from electrons to PS protons or from electrons to PC protons.

## TIME DEPENDENCE OF THE SOLID-EFFECT TRANSFER

For irradiation at the difference of the electron and proton Larmor frequencies, the time dependence of the positive DNP enhancement of proton polarization is described by:

$$\frac{dP_I}{dt} = -N_S W (P_I - P_S) - \frac{1}{T_I} (P_I - P_I^0) \quad (1)$$

$$\frac{dP_S}{dt} = -N_I W (P_S - P_I) - \frac{1}{T_S} (P_S - P_S^0) \quad (2)$$

These are Equations (10) and (11) in I, where definition of terms may be found. Under most experimental conditions pumping of microwave transitions is slow and the rate of change of the electron Zeeman population is small compared to that of the proton Zeeman population. Thus,

$$\frac{dP_S}{dt} = 0 \quad (3)$$

and

$$P_S = \frac{P_I + \frac{P_S^\circ}{N_I T_S W}}{1 + \frac{1}{N_I T_S W}} \quad (4)$$

Substitution of Equation (4) into Equation (1) and subsequent integration leads to:

$$P_I = \frac{1}{A} [B - C \exp(-At)] \quad (5)$$

where

$$A = ac + b \quad (6)$$

$$B = acP_S^\circ + bP_I^\circ \quad (7)$$

$$C = B - AP_I^\circ \quad (8)$$

and

$$a = \frac{1}{T_S \left\{ 1 + \frac{1}{N_I T_S W} \right\}} \quad (9)$$

$$b = \frac{1}{T_I} \quad (10)$$

$$c = \frac{N_S}{N_I} \quad (11)$$

Thus,  $P_I$  is  $P_I^\circ$  at the start of the microwave irradiation when  $t = 0$ , and then approaches the DNP enhancement of  $B/A$  (which is also given by Equation (13) of Paper I) exponentially in time with a rate constant,  $A$ . Equations (6, 9-11) show that in principle, this *microscopic* rate constant is always

greater than  $T_1^{-1}$ . However, in practice sometimes the initial rate of growth of the observed DNP enhancement appears to be less than  $T_1^{-1}$ . This occurs because many of the protons that are coupled to electrons and involved in the solid-effect transfer are frequency shifted from other protons. The frequency-shifted protons are not part of the detected signal, and have their own  $T_1$ 's which are longer than the bulk  $T_1$ . (A specific example is described in IV.) The observed *macroscopic* growth rate is therefore a composite process that involves electron-proton polarization transfer via H-H spin diffusion to nearby protons less tightly coupled to the electron and more easily detected. The *net* growth rate includes additional spin diffusion to all other more remote protons in the sample. These two diffusion processes are distinct; the first is between protons whose resonance frequencies are mismatched, while the second is between protons whose resonance frequencies are matched. In the following section, we describe the first process phenomenologically and the second process as Fickian diffusion.

## ONE-DIMENSIONAL FICKIAN DIFFUSION WITH SPIN-LATTICE RELAXATION FROM A POINT SOURCE OF MAGNETIZATION

We model the transfer of DNP-enhanced polarization to remote, frequency-matched protons as one-dimensional Fickian diffusion with spin-lattice relaxation (Figure 1). Protons contributing to the source of magnetization are near the free-radical center. For computational purposes, we replace the standard differential equation involving the diffusivity constant,  $D$ ,

$$\frac{\partial u(t,x)}{\partial t} = D \frac{\partial^2 u(t,x)}{\partial x^2} \quad (12)$$

with a difference equation [1],

$$\frac{1}{h}(u_{ij} - u_{i-1,j}) = \frac{D}{k^2}(u_{i-1,j+1} - 2u_{i-1,j} + u_{i-1,j-1}) \quad (13)$$

in which  $h$  and  $k$  scale the size of the time and space steps, and  $i$  and  $j$  are the difference-equation time and space variables, respectively. We add spin-lattice relaxation to obtain:

$$\begin{aligned} u_{ij} = u_{i-1,j} + \lambda \{ & [D(x_j + \frac{k}{2})][u_{i-1,j+1} - u_{i-1,j}] \\ & - [D(x_{j-1} + \frac{k}{2})][u_{i-1,j} - u_{i-1,j-1}] \\ & - [1 - \exp(-(i-1)/T_1(x_j + \frac{k}{2}))][u_{i-1,j}] \} \end{aligned} \quad (14)$$

Because polarization can cross the PC/PS interface, the diffusivity  $D$  and the proton spin-lattice relaxation time  $T_1$  depend on position in Equation (14). That is,

$$\begin{aligned} D &= D(x_j) \\ T_1 &= T_1(x_j) \end{aligned} \quad (15)$$

If there are  $T$  time steps of size  $h$ , and  $X$  space steps of size  $k$ , then,

$$\begin{aligned} i &= 1, 2, 3, \dots T \\ j &= 1, 2, 3, \dots X \end{aligned} \quad (16)$$

and  $x_j = j \cdot k$  (17)

The scaling ratio in Equation (14) is given by  $\lambda$  where

$$\lambda = \frac{h}{k^2} \quad (18)$$

The boundary conditions reflect the macroscopic growth of (normalized) DNP-enhanced polarization

$$u_{i,0} = [1 - \exp(-\alpha \cdot i)] \quad (19)$$

$$u_{0,j} = 0 \quad (20)$$

Equation (19) has the same form as Equation (5); thus,  $\alpha$  is a phenomenological rate constant that describes the composite process of solid-effect transfer from electrons to protons, plus H-H spin diffusion between protons with mismatched Larmor frequencies.

The diffusion Equation (14), with the boundary conditions given by Equations (19-20), was solved numerically on a microcomputer. The solution was obtained with  $T = 100$ ,  $X = 20$ , and the diffusivities and spin-lattice relaxation times of Table I. A value of  $1.5 \text{ sec}^{-1}$  was chosen for  $\alpha$  in Equation (19). This rate matches the growth in the DNP enhancement for the residual protons in PC( $^{13}\text{C}$ )/PS( $^{2}\text{D}/^*$ ) (I). Based on the  $\tau_c$ 's (time constants for H-H spin exchange) and  $D$ 's of Table I, each increment in  $x_j$  (Equation 17) represents 30 Å. Polystyrene has a density of 1.05 g/cc. Taking 15 Å as an approximate linear dimension for BDPA means that for



2% doping by weight, the average distance between uniformly dispersed free-radical centers is approximately 70 Å. Calculated polarization concentration profiles are shown in Figure 2. The top row shows the polarization concentration gradient in PS and the bottom row the gradient in PC. The calculation assumed changes in  $D$ 's and  $T_1$ 's from PS to PC values, two steps or 60 Å from the BDPA source of polarization in the PS phase.

## EXPERIMENTS

*BDPA-doped PS and Perdeuterated PS:* The BDPA-doped PS is the sample described in I. Perdeuterated styrene, 98%  $d_8$ -styrene, was purchased from Merck Stable Isotopes (Montreal, Canada) and was thermally polymerized to PS. The BDPA-doped perdeuterated PS sample, PS( $^2D$ /\*), was prepared in the same way as was BDPA-doped PS (I). DNP enhancements for doped homopolymers were measured as described in I.

*Thin-Film Blends:* A thin-film blend of  $^{13}C$ -enriched PC and BDPA-doped 98% perdeuterated PS, denoted as PC( $^{13}C$ )/PS( $^2D$ /\*), was prepared in a manner identical to that used to prepare the thin-film blend of  $^{13}C$ -enriched PC and BDPA-doped,  $^{13}C$ -depleted PS. Comparisons were made of the difference spectra of PC( $^{13}C$ )/PS( $^2D$ /\*) and PC( $^{13}C$ )/PS( $^{12}C$ /\*) obtained using the DNP CPMAS  $^{13}C$  NMR experiment described in I. These comparisons were of the results of experiments performed under identical conditions: the spectra were obtained back-to-back using the same microwave power of 5 watts and exactly 12000 scans for each experiment. The CPMAS spectrum of PS(\*) was subtracted from the DNP difference

spectrum of PC( $^{13}\text{C}$ )/PS( $^{2}\text{D}/*$ ) to remove the contribution of the residual natural-abundance  $^{13}\text{C}$  phenyl-ring carbons of PS( $^{2}\text{D}$ ) from the difference signal. The PS( $*$ ) spectrum was scaled so that the aliphatic-carbon signal in the PC( $^{13}\text{C}$ )/PS( $^{2}\text{D}/*$ ) spectrum was matched.

The DNP CPMAS  $^{13}\text{C}$  NMR experiment was done on the thin-film blend PC( $^{13}\text{C}$ )/PS( $^{12}\text{C}/*$ ) with varying microwave-irradiation times. The microwave irradiation times varied from 0.4 to 2.0 seconds. The sequence of the irradiation times was 2.0, 0.4, 1.6, 0.8, 1.2, 0.6, 1.0, 1.8, and 1.4 seconds, respectively. A total of nine files corresponding to nine different irradiation times, each containing about 3000 scans, were collected and the experiment was repeated six times for a total of 18000 scans for each microwave-irradiation time. In order to avoid a droop in microwave power during the experiment due to aging of the klystron, the microwave power level was intentionally set at a value lower than the maximum available power. At the time of this experiment the maximum available power was 4 watts, and the experiment was performed at 2.5 watts. Doing the experiment at lower power levels had the advantage that the interfacial-PC signals were relatively well resolved making quantitation easier.

## RESULTS

*DNP of Protons in BDPA-Doped PS and Perdeuterated PS:* The proton NMR spectra of the residual protons in 98% perdeuterated polystyrene, PS( $^{2}\text{D}$ ), obtained by using a standard proton solid-echo experiment, are well enough resolved that aromatic- and aliphatic-proton signals can be distinguished (Figure 3, bottom). Spinning sidebands extending over about

$\pm 6$  kHz arise from  $^1\text{H}$ - $^2\text{D}$  and residual  $^1\text{H}$ - $^1\text{H}$  inhomogeneous dipolar coupling [2].

When the perdeuterated PS sample is doped with 2% by weight BDPA, the proton linewidth (full width at half maximum) increased to 1.3 kHz for the residual protons. The aromatic- and aliphatic-proton resonances are not resolved (Figure 3, top). This broadening is due to dipolar coupling to the unpaired electrons in BDPA ( $T_{1e} = 750 \mu\text{s}$ ). The proton linewidth of 1.3 kHz is a factor of 20 less than that of the fully protonated PS but a factor of five greater than susceptibility broadening. An upper limit for the susceptibility broadening is assessed by the  $^{13}\text{C}$  linewidth in a similarly doped sample (Figure 3, insert). The insert in Figure 3 is the CPMAS  $^{13}\text{C}$  NMR spectrum of PC( $^{13}\text{C}$ )/PS( $^2\text{D}/^*$ ).

The positive DNP enhancement observed for PS( $^*$ ) using the proton solid-echo experiment is a factor of 20 for 10-watts microwave power applied for 2 seconds (I). For 5-watts microwave power, the DNP enhancement for PS( $^*$ ) reaches a value of about 10 in 1 second, while that for the residual protons in PS( $^2\text{D}/^*$ ) reaches the same value but requires twice the microwave pumping time (Figure 4). The enhancement in PS( $^2\text{D}/^*$ ) has not quite reached a plateau after 2 seconds of microwave irradiation. The extrapolated, infinite-power enhancement of PS( $^2\text{D}/^*$ ) is about 1.5 times larger than that of PS( $^*$ ).

*DNP of Thin-Film Blends:* A comparison of the integrated intensities of the DNP-enhanced interface signal from PC( $^{13}\text{C}$ )/PS( $^2\text{D}/^*$ ) and PC( $^{13}\text{C}$ )/PS( $^{12}\text{C}/^*$ ) shows that the two thin-film blend samples give rise to about the same PC integrated intensity (Figure 5, top and bottom inserts).

The interface-PC signal and the unenhanced, standard CPMAS  $^{13}\text{C}$  NMR signal of bulk PC in this particular PC( $^{13}\text{C}$ )/PS( $^{2}\text{D}/^*$ ) thin-film blend are both broadened by an inhomogeneous local susceptibility effect. This result was established from echo intensities in rotor-synchronized, Carr-Purcell refocusing experiments which are described in III.

Although, the DNP-enhanced bulk PC  $^1\text{H}$  and  $^{13}\text{C}$  signal intensities in PC( $^{13}\text{C}$ )/PS( $^{12}\text{C}/^*$ ) increase monotonically, the DNP-enhanced interface PC signal reaches a maximum after about 1.2-seconds microwave pumping and then decreases. The DNP CPMAS  $^{13}\text{C}$  difference spectra for 0.4, 1.2, and 2.0-seconds microwave irradiation times are shown in Figure 6. The complete dependence of the intensity of the DNP-enhanced PC interface signal as a function of the microwave irradiation time is shown in Figure 7 (solid circles, right panel).

## DISCUSSION

*Mechanism of Polarization Transfer in PS and Perdeuterated PS:* The dominant transfer mechanism in BDPA-doped polystyrene is a direct electron-to-proton solid-effect enhancement. Proton-proton spin diffusion helps to redistribute polarization but is not essential. Disruption of H-H spin diffusion by deuteration does not reduce the DNP-enhancement factor (Figure 4). Because spin diffusion allows polarization to move 50-100 Å in one second in fully protonated PS [2], and because deuteration of PS only slows reaching full DNP enhancement for the residual protons but not the enhancement itself, we conclude that the electron-proton solid effect operates over distances comparable to 50 Å. This conclusion is consistent

with the linear dependence of DNP enhancement with microwave power shown in I (Figure 7). With one electron per 2000 protons in fully protonated PS, and with electrons separated by less than 100 Å, sizable DNP enhancements can be generated by direct electron-to-proton polarization transfers even with  $T_{1e}$ 's of one msec.

Any contribution of spin diffusion to the observed DNP enhancement in PS(<sup>2</sup>D/\*) still involves a slow transfer under frequency-mismatched conditions, from protons directly polarized by a solid-effect transfer to nearby protons. More distant protons are, however, not polarized by the fast spin diffusion illustrated in panels 2 and 3 of Figure 2, but rather are directly polarized by a slower version of the solid-state composite process represented by panel 1. The resulting distribution of transfer rates explains the absence of a plateau for the DNP enhancement of PS(<sup>2</sup>D/\*) in Figure 4.

*Mechanism of Polarization Transfer in PC/PS Thin-Film Blends:* The positive proton polarization generated by microwave pumping of PC(<sup>13</sup>C)/PS(<sup>12</sup>C/\*) at the difference of the electron and proton Larmor frequencies can cross the PC/PS boundary either by H-H dipolar contact between protons of PC and PS and spin diffusion, or by direct solid-effect enhancement of PC protons by electrons in PS phase, or by a combination of the two pathways. This situation is illustrated in Figure 8.

Because removal of at least 98% of the protons on the PS side of the PC/PS interface in thin-film blends has no effect on the integrated intensity of the interface-PC signal (Figure 5), the dominant solid-effect transfer is from electrons in the PS phase that are of the order of 50 Å from the interface to protons in the PC phase. Based on the PS(<sup>2</sup>D/\*) results

discussed above, we know that direct transfers over these distances occur. In fact, we believe that the narrow carbon linewidth observed for low-power microwave irradiation (Figure 14, I) arises because more distant protons avoid frequency-mismatched polarization-transfer bottlenecks and so are the first to be detected.

The DNP-enhanced interface-PC signal intensity is 4% of the unenhanced bulk-PC signal intensity in the thin-film PC(<sup>13</sup>C)/PS(<sup>12</sup>C/\*) blend. Taking into account the DNP enhancement factor of 2 for PC protons at half microwave power (I, Figure 7), the interface PC signal is qualitatively consistent with a 60-Å thick interface, or about 2% of the 3000-Å thick PC thin film. In comparing interface-PC signals to bulk-PS signals, the <sup>13</sup>C isotopic enrichment of PC at the interface offsets the ratio of interface material to bulk material. Therefore, because the solid-effect enhancement for PS protons is five times that of PC protons (I), we expect the bulk-PS, aliphatic-carbon signal intensity ( $\delta_C$  45) to be about five times that of the interface-PC, aromatic-carbon signal ( $\delta_C$  120). Experiment shows a ratio of approximately five-to-one (Figure 5, bottom).

We believe that the observed decrease in PC polarization with increasing time of microwave irradiation (Figure 6) may be due to a shortening of the PC  $T_1(H)$  by local inductive heating. Faster PC spin-lattice relaxation would increase spin-lattice polarization leakage and thus reduce the enhancement. Another explanation involving spin diffusion is offered below.

*Spin Diffusion Across the Interface of the PC-Protonated PS Blend:* Even though inductive heating is a plausible explanation for the maximum in the

interface PC signal with microwave irradiation, we cannot eliminate spin diffusion as a minor contributor. The results of the calculation of Figure 2 show that polarization originating in the fully protonated PS phase can reach and cross the interface to the PC phase. However, the calculation shows a plateau for PC polarization with increasing time of microwave irradiation rather than the observed decrease (Figure 6). We find that we can account for such a decrease by the calculation only if we reduce  $D$  and  $T_1(H)^{-1}$  of both PS and PC by a factor of about 100 relative to  $\alpha$  (Figure 9). With slower spin diffusion, the effect of relaxation has time to accumulate thereby altering the shapes of the concentration profiles. As long as we maintain the same ratios of  $D$ 's to  $T_1(H)^{-1}$ 's as in Table I, the total PC interface polarization is comparable to that of the calculation of Figure 2. But now the calculated time dependence of interface polarization in PC matches the observed maximum near  $t = 1.5$  sec (Figure 7, right). The step size of the difference-equation calculation still corresponds to  $30 \text{ \AA}$  if the time constant for H-H spin exchange,  $\tau_c$  (Table I), has also increased by a factor of a 100.

We can rationalize the reductions in  $D$ 's as due to frequency offsets arising from variations in dipolar coupling to free electrons near the interface, and those in  $T_1(H)^{-1}$ 's as due to a balancing of Zeeman relaxation by a direct, long-range solid-effect enhancement. However, adopting this rationalization implies that electron-to-proton transfers are indeed long range and so can cross the PC/PS interface directly without the assistance of spin diffusion.

## ACKNOWLEDGEMENTS

The perdeuterated polystyrene was synthesized by R.J. Kern (Monsanto Company, St Louis). This work has been supported by the Office of Naval Research under contract N00014-88-K-0183.



**Table I** Parameters for Fickian Diffusion Calculations

	<u>Polystyrene</u>	<u>Polycarbonate</u>
$H_L$ , kHz <sup>a</sup>	8	4
$\tau_C(1.5 \text{ \AA})$ , msec <sup>b</sup>	0.04	0.08
$1/\tau_C(30 \text{ \AA})$ , sec <sup>-1</sup> <sup>c</sup>	50	25
$D$ , 10 <sup>-12</sup> cm <sup>2</sup> /sec <sup>d</sup>	4.50	2.25
$T_1(H)$ , sec <sup>e</sup>	1	0.1

<sup>a</sup>From experiment, Ref. [3]. Molecular motion reduces  $H_L$  in PC.

<sup>b</sup>From  $\tau_C = 1/\pi H_L$ , assuming an average interproton distance of 1.5 Å.

<sup>c</sup>From  $\tau_C(30 \text{ \AA}) = 400 \tau_C(1.5 \text{ \AA})$ .

<sup>d</sup>From  $D = \langle x \rangle^2 / \tau_C$

<sup>e</sup>From experiment, this work.

## REFERENCES

1. Crank, J. in *Mathematics of Diffusion*, Chap. X, Oxford University Press, Oxford, 1956.
2. VanderHart, D.L.; Manders, W.F.; Stein, R.S.; Herman, W. *Macromolecules*, 1987, 20, 1724.
3. Schaefer, J.; Sefcik, M.D.; Stejskal, E.O.; McKay, R.A. *Macromolecules*, 1981, 14, 280.

## FIGURE CAPTIONS

Figure 1. Hypothetical polarization gradient resulting from H-H spin diffusion away from a source of DNP-enhanced magnetization in a free-radical doped polymer with variable  $^1\text{H}$   $T_1$ 's and  $T_2$ 's. The source of magnetization is protons near the free-radical centers but with resonance frequencies matched to that of the bulk protons. The dotted line indicates a compositional change in the medium such as that which occurs at the interface between PC and PS in thin-film heterogeneous blends.

Figure 2. Calculated concentration profiles resulting from frequency-matched H-H spin diffusion with spin-lattice relaxation (panels 2-6) away from a source of magnetization (panel 1). The calculation is the solution to Equation (4.14) with the boundary conditions of Equations (4.19, 4.20), the parameters of Table 1, and  $\alpha = 1.5 \text{ sec}^{-1}$ . The top row represents the polarization gradient in BDPA-doped PS and the bottom row the polarization gradient in the BDPA-free PC in a heterogeneous thin-film blend. Each panel represents a  $30\text{-\AA}$  step away from the magnetization source which is protons polarized by a direct solid-effect transfer from electrons. The PC/PS interface is  $60 \text{ \AA}$  from the magnetization source.

Figure 3. 1.4-T solid-echo  $^1\text{H}$  NMR spectrum of the residual protons in 98% perdeuterated PS spinning at the magic angle at 1859 Hz (bottom). Signals from aromatic and aliphatic protons are resolved. Spinning sidebands are due primarily to heterogeneous  $^1\text{H}$ - $^2\text{D}$  and  $^1\text{H}$ - $^1\text{H}$  dipolar coupling. The DNP-enhanced  $^1\text{H}$  NMR spectrum from BDPA-doped perdeuterated PS has similar spinning sidebands but is less well resolved (top). Contributions to

the  $^1\text{H}$  linewidth from local susceptibility variations are no more than 20%, based on the 1.4-T  $^{13}\text{C}$  linewidth in a  $\text{PC}(^{13}\text{C})/\text{PS}(^2\text{D}/^*)$  blend (insert, top left).

Figure 4. DNP enhancement of the  $^1\text{H}$  NMR signal intensity as a function of the microwave-irradiation time for  $\text{PS}(^*)$  and  $\text{PS}(^2\text{D}/^*)$ .

Figure 5. DNP-difference  $^{13}\text{C}$  NMR spectra of thin-film blends of  $\text{PC}(^{13}\text{C})/\text{PS}(^{12}\text{C}/^*)$  (bottom) and  $\text{PC}(^{13}\text{C})/\text{PS}(^2\text{D}/^*)$  (top two inserts). The spectra in the inserts arise both from natural-abundance carbons coupled to the residual protons in perdeuterated bulk PS, and from label in  $^{13}\text{C}$ -enriched interface PC.

Figure 6. DNP difference  $^{13}\text{C}$  NMR spectra of  $\text{PC}(^{13}\text{C})/\text{PS}(^{12}\text{C}/^*)$  as a function of the microwave-irradiation time. The DNP enhancement for interface PC reaches a maximum after irradiation for about 1.2 seconds, while that of the bulk PS monotonically increases with the microwave-irradiation time. The horizontal dashed lines indicate signal levels for 1.2-second microwave-irradiation times.

Figure 7. Relative DNP-difference  $^{13}\text{C}$  NMR signal intensities as a function of microwave-irradiation time for bulk PS (left) and total interface PC in  $\text{PC}(^{13}\text{C})/\text{PS}(^{12}\text{C}/^*)$ . Circles are experimental points. Solid curves were calculated from a Fickian diffusion model (with spin-lattice relaxation) of spin diffusion using the parameters of Figure 9.

Figure 8. Polarization transfer from electrons (stars) to protons in the undoped phase of a two-phase heterogeneous blend can occur directly or indirectly, the latter by  $^1\text{H}$ - $^1\text{H}$  spin diffusion.

Figure 9. Similar calculated concentration profiles to those described in the caption to Figure 4.2 but with  $D = 9 \times 10^{-14}$  cm<sup>2</sup>/sec and  $T_1 = 200$  sec for PS (top row);  $D = 4.5 \times 10^{-14}$  cm<sup>2</sup>/sec,  $T_1 = 40$  sec for PC (bottom row); and  $\alpha = 1.5$  sec. The anomalously slow spin diffusion is assumed to result from Larmor-frequency offsets (mismatches) arising from dipolar coupling to free electrons near the interface. Slow spin-lattice relaxation is assumed to result from Zeeman pumping by a local, direct solid-effect DNP enhancement.

# ONE-DIMENSIONAL FICKIAN DIFFUSION

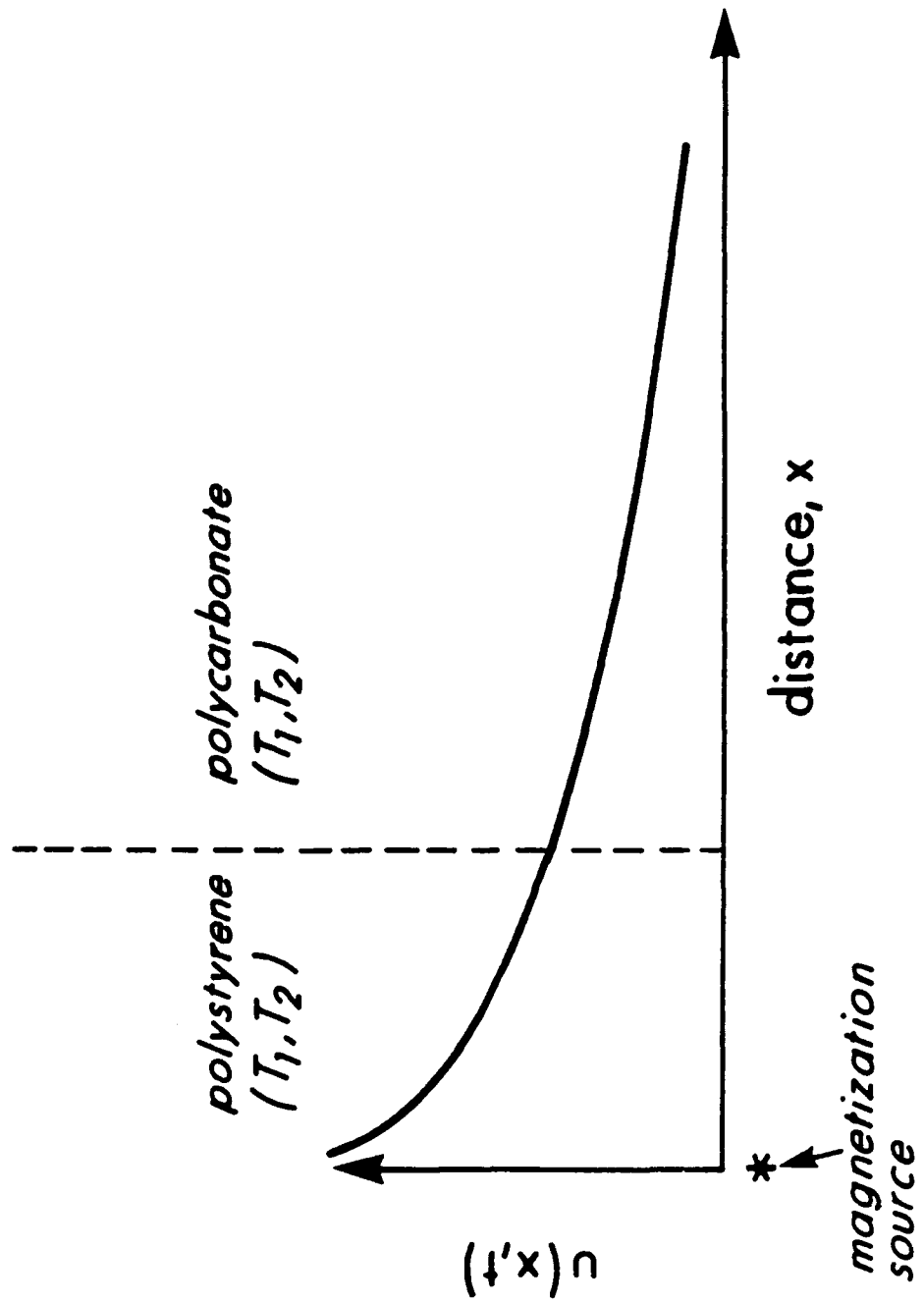


Figure 1

**DIFFUSION OF MAGNETIZATION (with relaxation)  
AWAY FROM SOURCE**

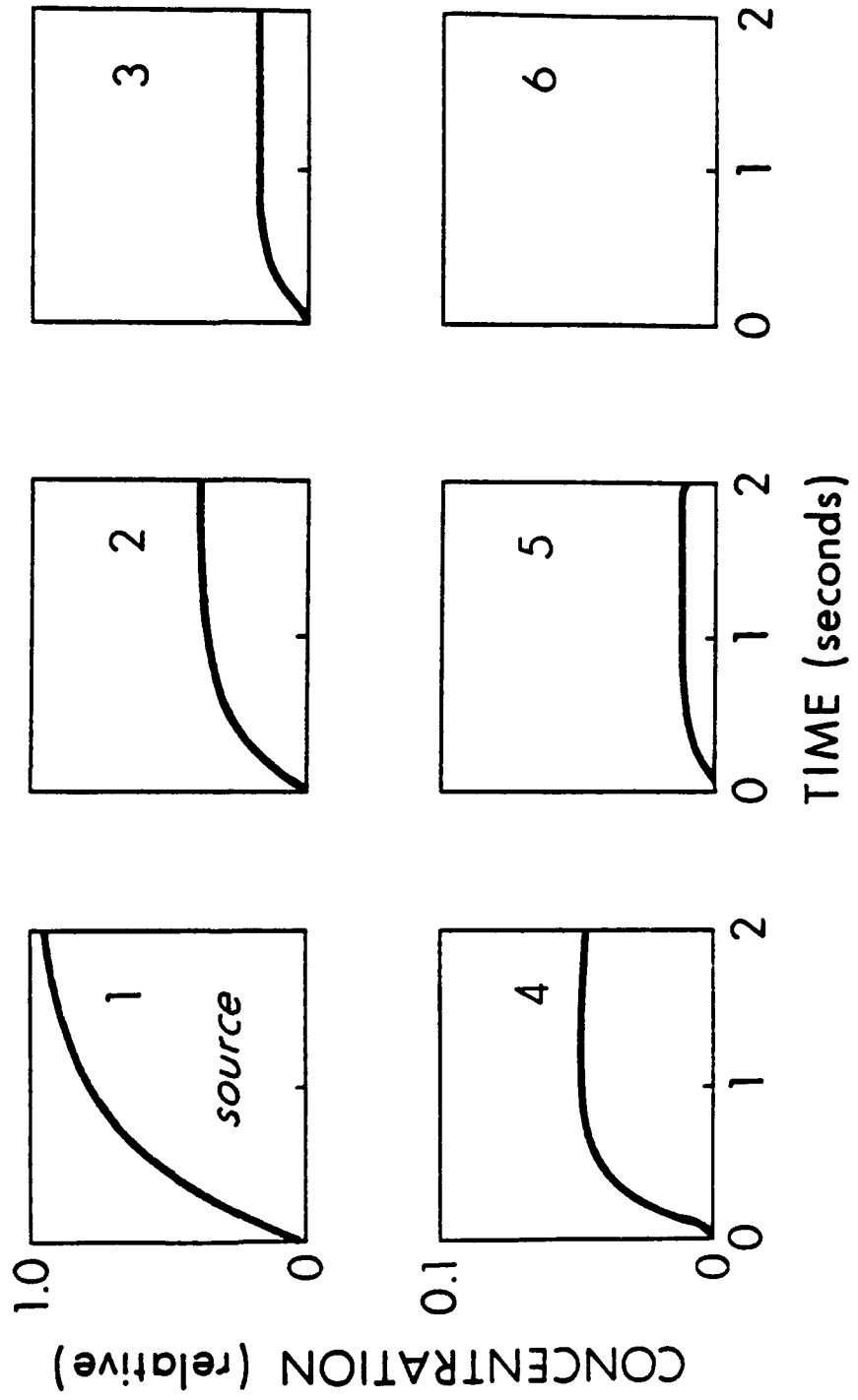


Figure 2

Figure 3

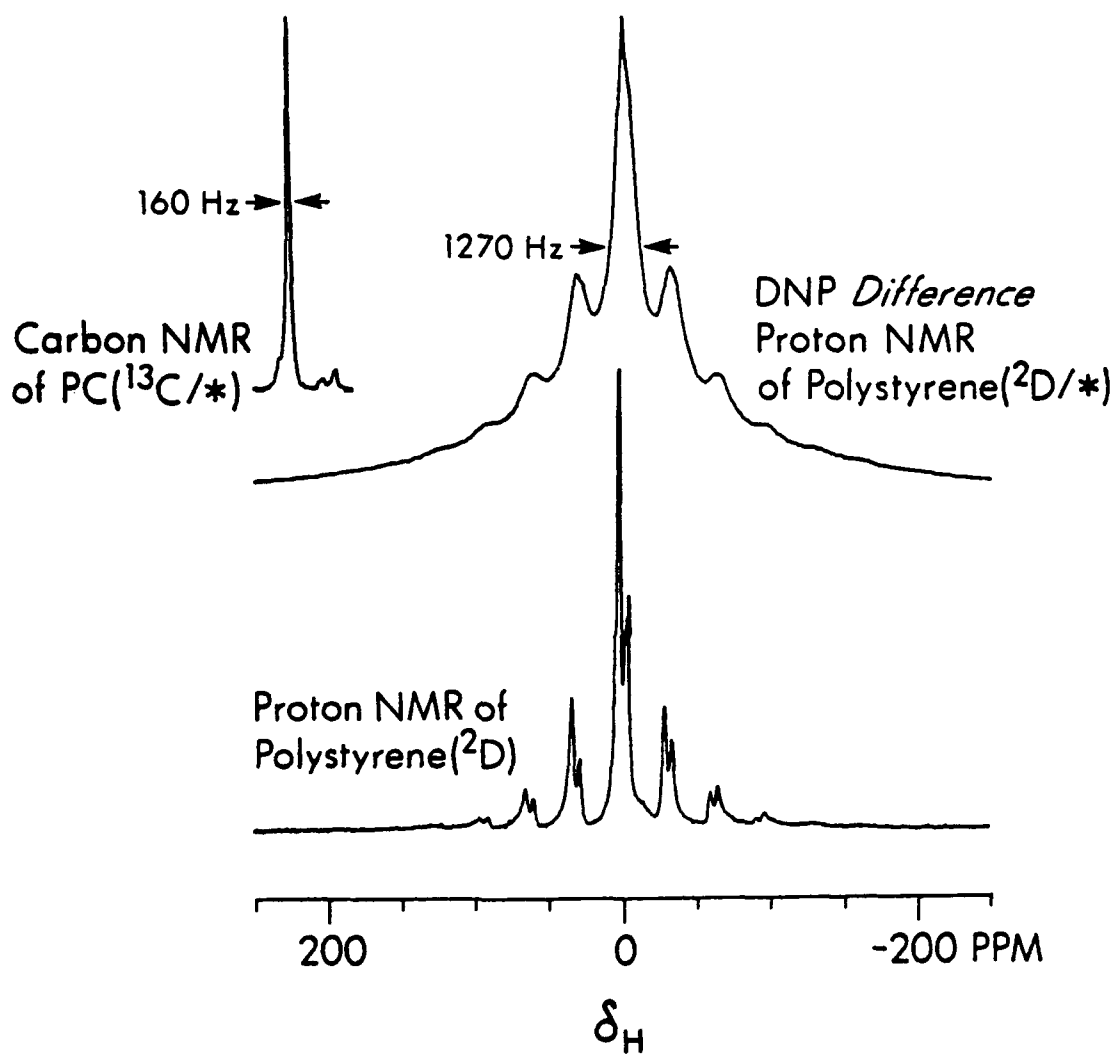




Figure 4

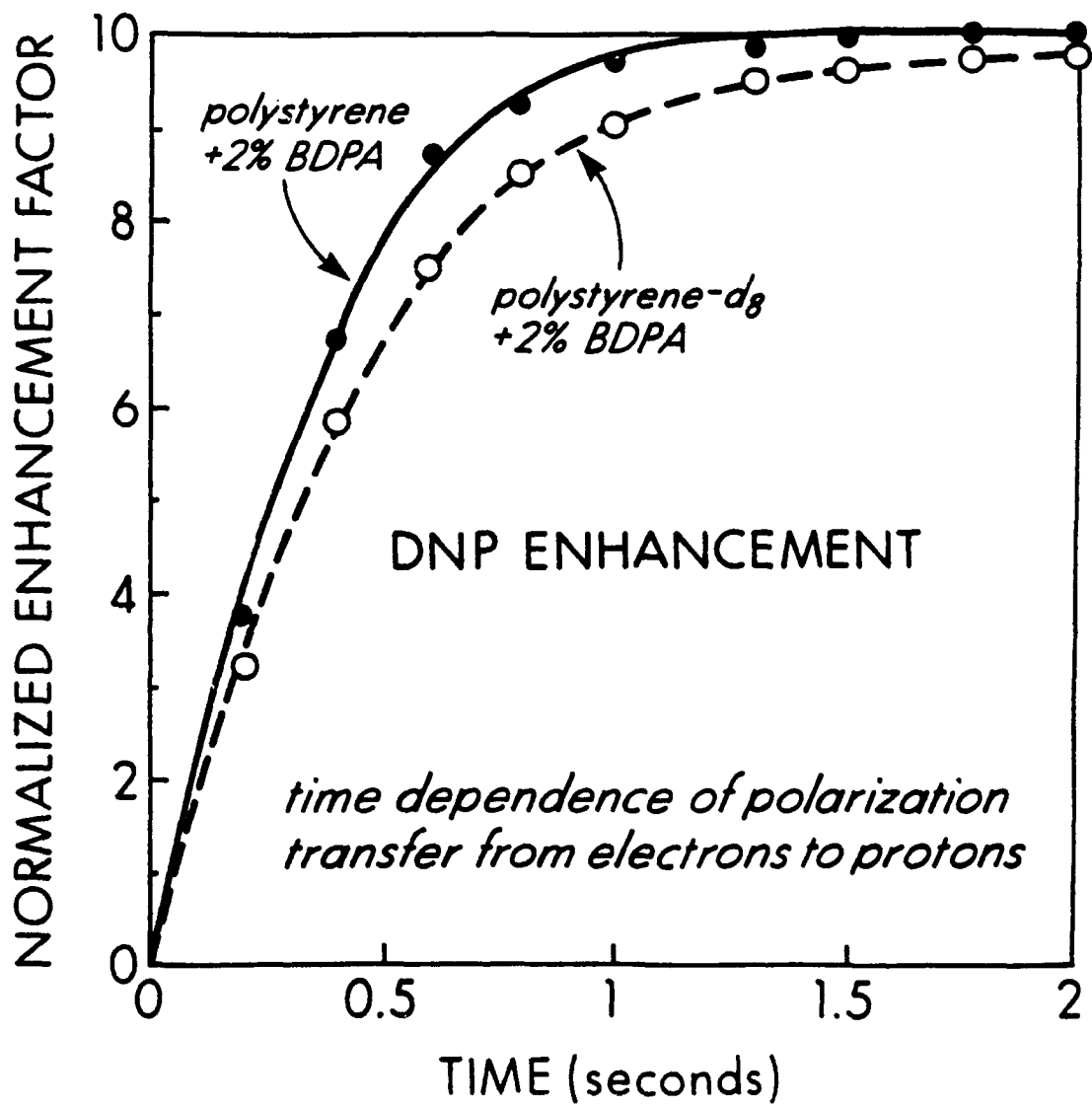


Figure 5

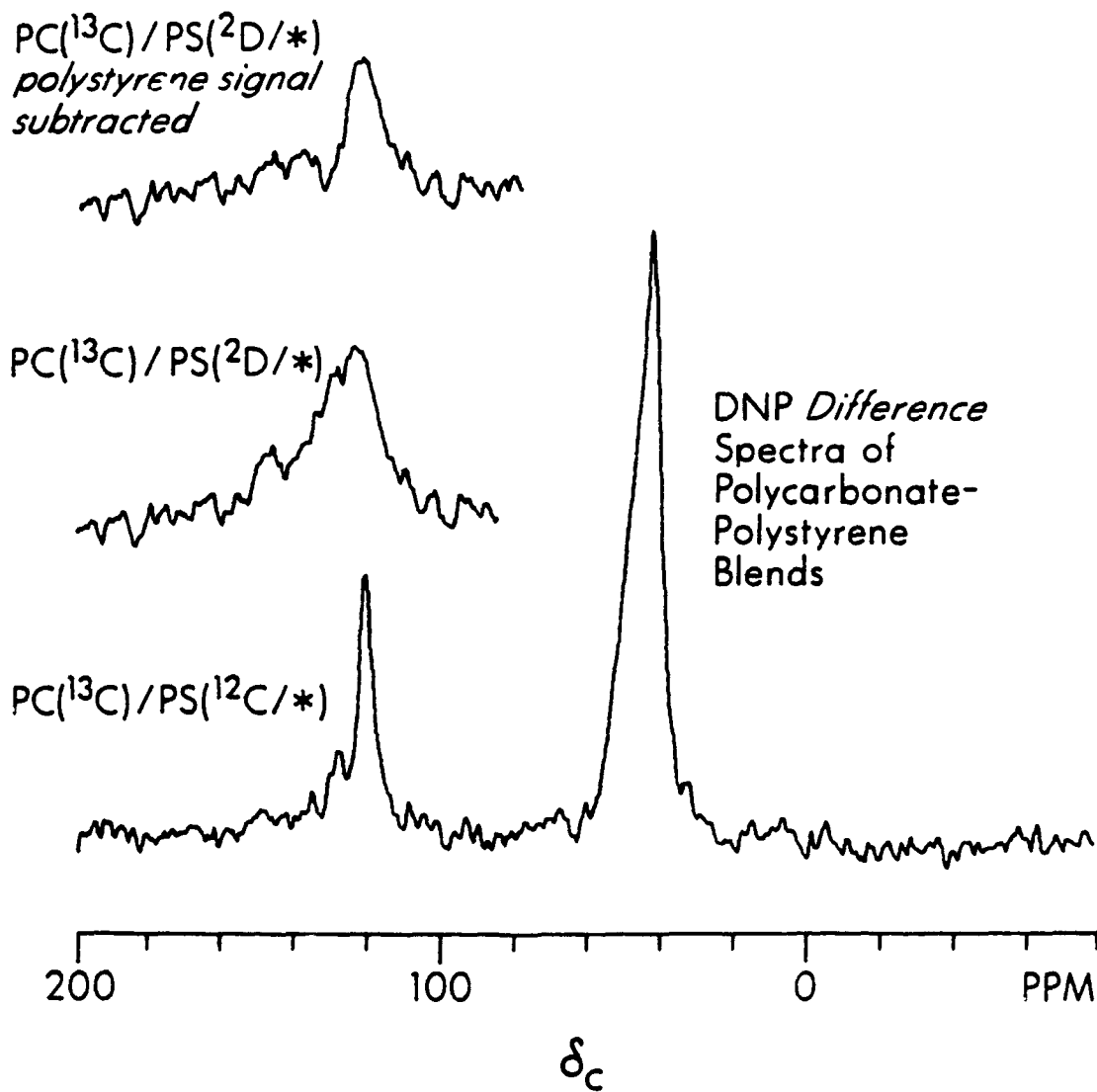
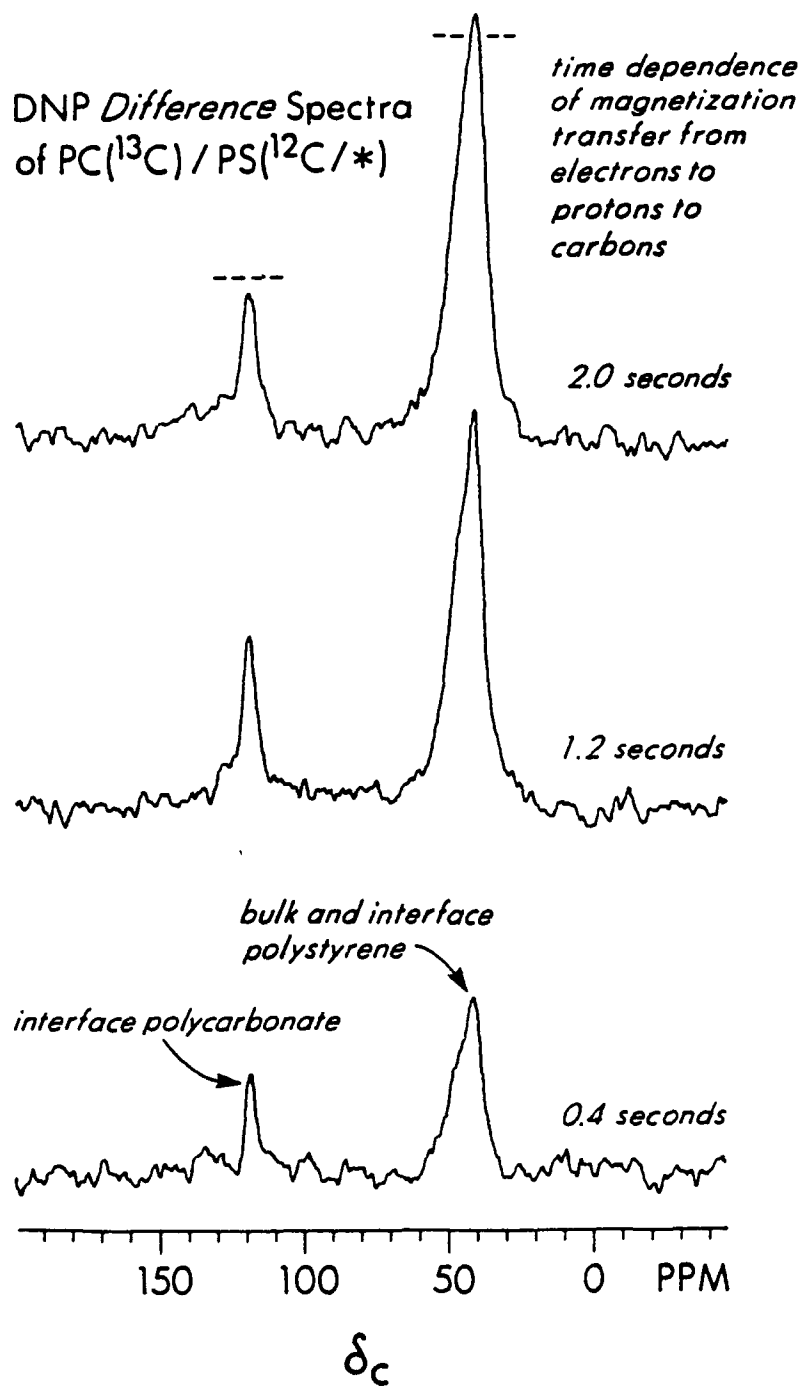


Figure 6



DNP DIFFERENCE OF PC(<sup>13</sup>C)/PS(<sup>12</sup>C/\*)

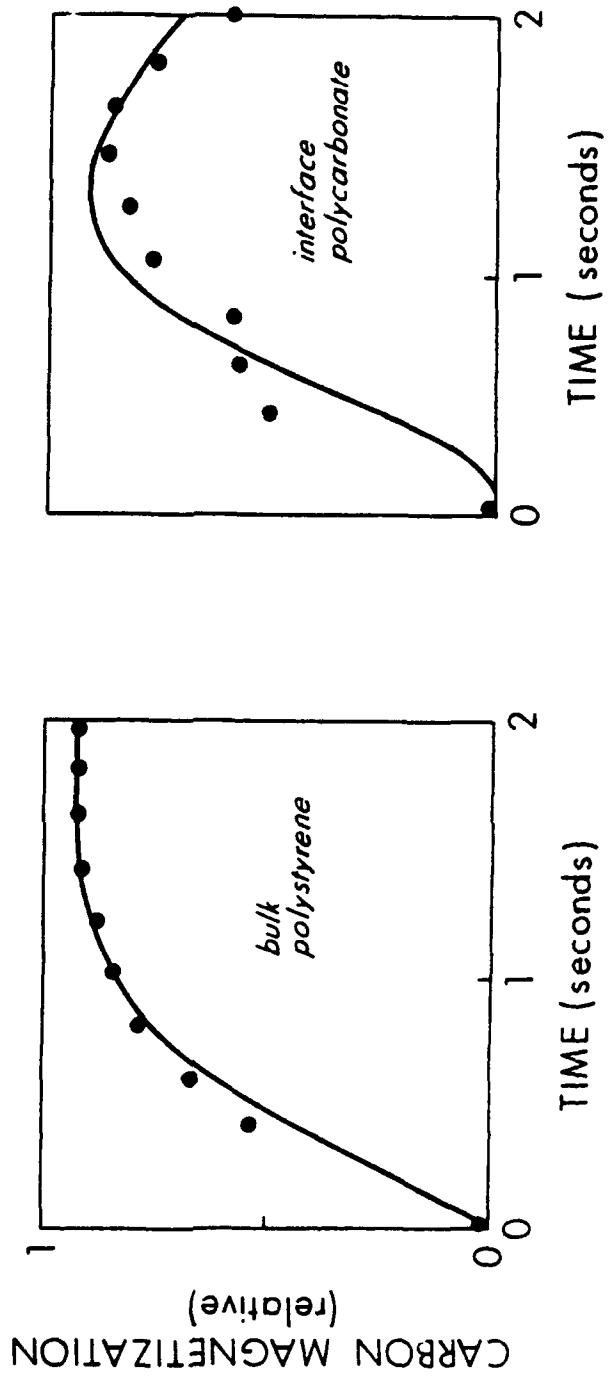


Figure 7

# TWO MODES OF POLARIZATION TRANSFER

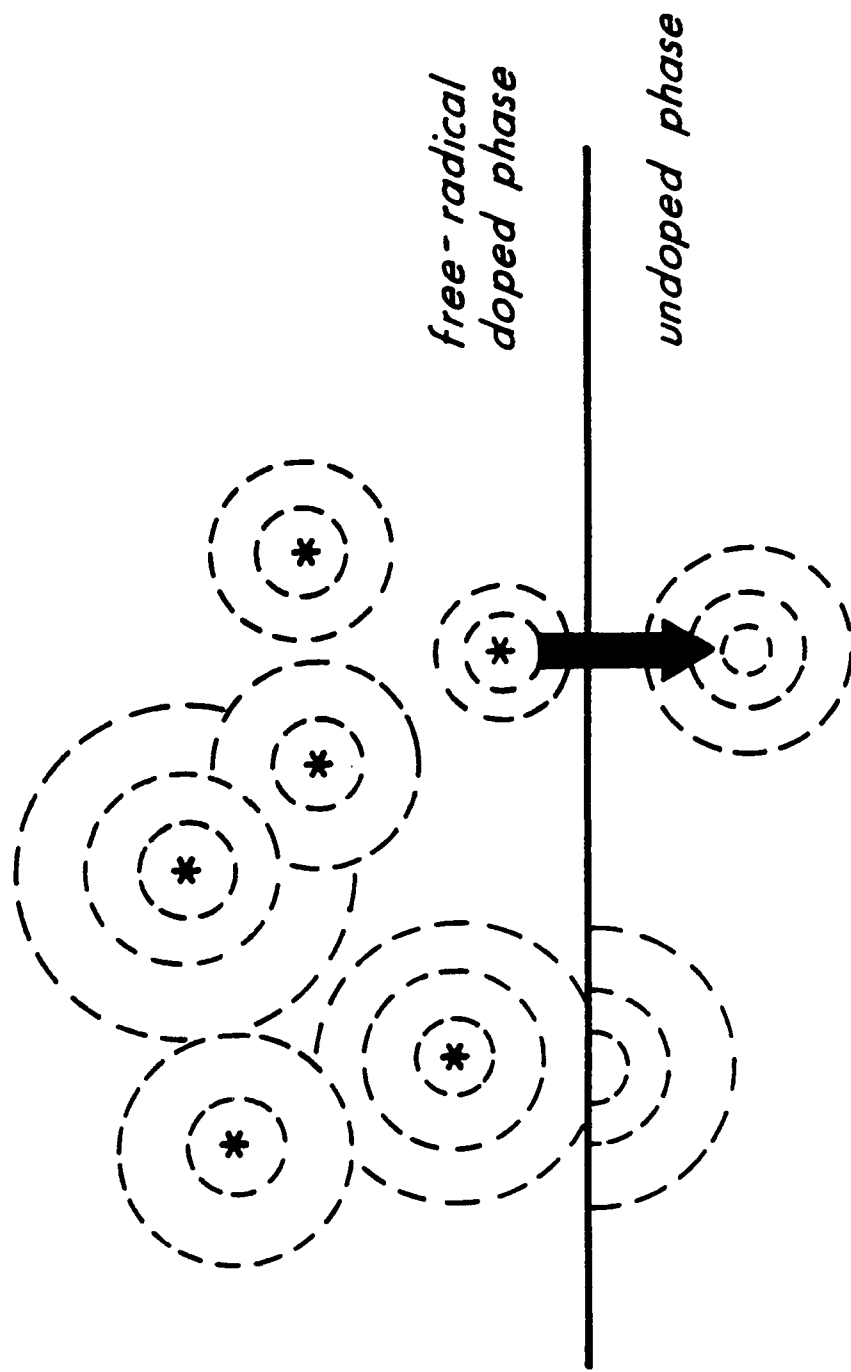


Figure 8

DIFFUSION OF MAGNETIZATION (with relaxation) AWAY FROM SOURCE

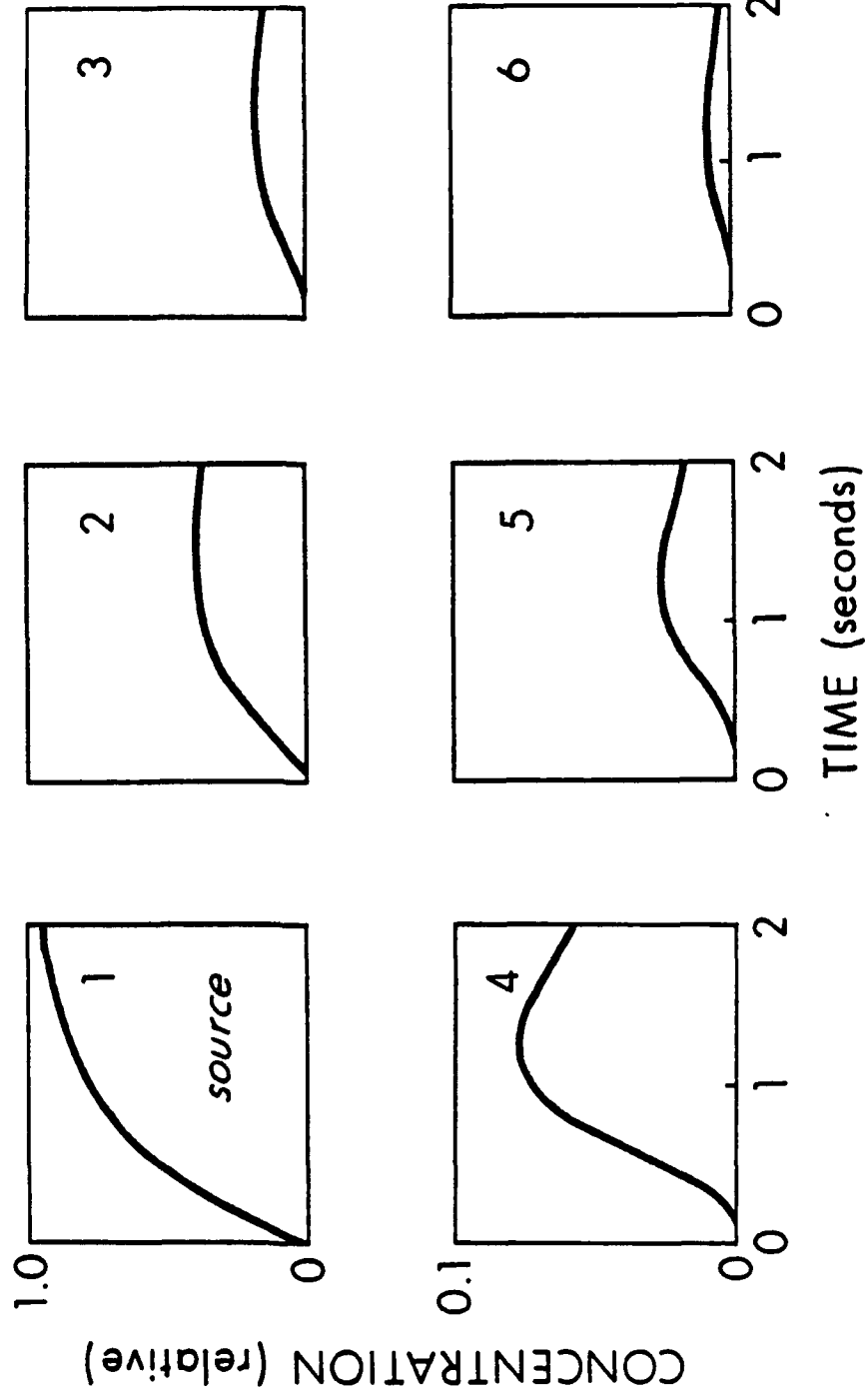


Figure 9

TECHNICAL REPORT DISTRIBUTION LIST - GENERAL

Office of Naval Research (2) Chemistry Division, Code 1113 800 North Quincy Street Arlington, Virginia 22217-5000	Dr. Robert Green, Director (1) Chemistry Division, Code 385 Naval Weapons Center China Lake, CA 93555-6001
Commanding Officer (1) Naval Weapons Support Center Dr. Bernard E. Douda Crane, Indiana 47522-5050	Chief of Naval Research (1) Special Assistant for Marine Corps Matters Code 00MC 800 North Quincy Street Arlington, VA 22217-5000
Dr. Richard W. Drisko (1) Naval Civil Engineering Laboratory Code L52 Port Hueneme, CA 93043	Dr. Bernadette Eichinger (1) Naval Ship Systems Engineering Station Code 053 Philadelphia Naval Base Philadelphia, PA 19112
David Taylor Research Center (1) Dr. Eugene C. Fischer Annapolis, MD 21402-5067	Dr. Sachio Yamamoto (1) Naval Ocean Systems Center Code 52 San Diego, CA 92152-5000
Dr. James S. Murday (1) Chemistry Division, Code 6100 Naval Research Laboratory Washington, D.C. 20375-5000	Dr. Harold H. Singerman (1) David Taylor Research Center Code 283 Annapolis, MD 21402-5067

In preparing the general distribution list for the TECHNICAL REPORTS, the address for the Defense Technical Information Center (DTIC) was omitted. When technical reports are prepared, two high quality copies should be forwarded to:

Defense Technical Information Center  
Building 5, Cameron Station (2)  
Alexandria, VA 22314